

Germline RBBP8 variants associated with early-onset breast cancer compromise replication fork stability

The COMPLEXO Network

DOI:
[10.1172/JCI127521](https://doi.org/10.1172/JCI127521)

License:
None: All rights reserved

Document Version
Peer reviewed version

Citation for published version (Harvard):
The COMPLEXO Network 2020, 'Germline RBBP8 variants associated with early-onset breast cancer compromise replication fork stability', *Journal of Clinical Investigation*, vol. 130, no. 8, pp. 4069-4080.
<https://doi.org/10.1172/JCI127521>

[Link to publication on Research at Birmingham portal](#)

Publisher Rights Statement:
<https://doi.org/10.1172/JCI127521>.
Copyright © 2020, American Society for Clinical Investigation

General rights

Unless a licence is specified above, all rights (including copyright and moral rights) in this document are retained by the authors and/or the copyright holders. The express permission of the copyright holder must be obtained for any use of this material other than for purposes permitted by law.

- Users may freely distribute the URL that is used to identify this publication.
- Users may download and/or print one copy of the publication from the University of Birmingham research portal for the purpose of private study or non-commercial research.
- User may use extracts from the document in line with the concept of 'fair dealing' under the Copyright, Designs and Patents Act 1988 (?)
- Users may not further distribute the material nor use it for the purposes of commercial gain.

Where a licence is displayed above, please note the terms and conditions of the licence govern your use of this document.

When citing, please reference the published version.

Take down policy

While the University of Birmingham exercises care and attention in making items available there are rare occasions when an item has been uploaded in error or has been deemed to be commercially or otherwise sensitive.

If you believe that this is the case for this document, please contact UBIRA@lists.bham.ac.uk providing details and we will remove access to the work immediately and investigate.

**Germline *RBBP8* variants associated with early-onset breast cancer
compromise replication fork stability**

Reihaneh Zarrizi^{1, #}, Martin R. Higgs^{2, #}, Karolin Voßgröne^{1, #}, Maria Rossing³, Birgitte Bertelsen³, Muthiah Bose¹, Arne Nedergaard Kousholt¹, Heike Rösner¹, The Complexo network, Bent Ejlersen⁴, Grant S. Stewart², Finn Cilius Nielsen^{3*}, Claus S. Sørensen^{1*}

¹Biotech Research and Innovation Centre, University of Copenhagen, Ole Maaløes Vej 5, Copenhagen 2200 N, Denmark.

²Institute of Cancer and Genomic Sciences, College of Medical and Dental Sciences, University of Birmingham, Birmingham, B15 2TT, UK.

³Centre for Genomic Medicine, Rigshospitalet, Copenhagen University Hospital, Blegdamsvej 9, Copenhagen 2100 Ø, Denmark.

⁴Department of Oncology, Rigshospitalet, Copenhagen University Hospital, Blegdamsvej 9, Copenhagen 2100 Ø, Denmark.

- First authors

*Correspondence:

Finn Cilius Nielsen; e-mail: Finn.Cilius.Nielsen@regionh.dk, Phone: 0045 3545

Claus S. Sørensen; e-mail: claus.storgaard@bric.ku.dk, Phone: 0045 3532 5678

The authors have declared that no conflict of interest exists.

23 **Abstract**

24 Haploinsufficiency of factors governing genome stability underlies hereditary breast and
25 ovarian cancer. Homologous recombination (HR) repair is a major pathway disabled in these
26 cancers. With the aim of identifying new candidate genes, we examined early-onset breast
27 cancer patients negative for *BRCA1* and *BRCA2* pathogenic variants. Here, we focused on
28 CtIP (*RBBP8* gene) that mediates HR repair through the end-resection of DNA double-strand
29 breaks (DSB). Notably, the patients exhibited a number of rare germline *RBBP8* variants, and
30 functional analysis revealed that these variants did not affect DNA DSB end-resection
31 efficiency. However, expression of a subset of variants led to deleterious nucleolytic
32 degradation of stalled DNA replication forks in a manner similar to cells lacking *BRCA1* or
33 *BRCA2*. In contrast to *BRCA1* and *BRCA2*, CtIP deficiency promoted the helicase-driven
34 destabilization of RAD51 nucleofilaments at damaged DNA replication forks. Taken together,
35 our work identifies CtIP as a critical regulator of DNA replication fork integrity, which when
36 compromised, may predispose to the development of early-onset breast cancer.

Introduction

Hereditary breast and ovarian cancer (HBOC) is causally linked with germline pathogenic variants in proteins implicated in homologous recombination repair (HRR), the protection of stalled DNA replication forks and cell cycle checkpoint control (1-6). *BRCA1* and *BRCA2* are the most commonly mutated genes in HBOC, accounting for approximately 15% of cases (7). However, a number of less frequent genetic alterations that predispose to breast cancer have been uncovered in other genes e.g. *RECQL1*, *PALB2* and *BRIP1* (3, 8-10). For the majority of emerging HBOC genes, it is currently not possible to provide accurate risk estimates because they are rare. This poses challenges to cancer risk management and counseling of women who carry variants in these genes as well as burdens their families. Consequently, it has been proposed that functional analyses should be employed in the classification of novel genetic variants (1).

Notably, genetic and functional analysis of breast cancer associated variants have uncovered substantial locus heterogeneity. Several HRR factors, other than *BRCA1* and *BRCA2*, increase the risk of breast cancer including *PALB2* and *RAD51C* (1, 8, 11). CtIP, encoded by the *RBBP8* gene, is a major HRR factor that has thus far not been functionally linked with HBOC. CtIP is a key regulator of double-strand break (DSB) resection operating within the *BRCA1/BRCA2* pathway, and generates the single-stranded DNA segment needed for *RAD51*-mediated recombination. Here, we examined a high-risk population of early-onset *BRCA1* and *BRCA2* mutation-negative breast cancer patients for germline variants in *RBBP8*. Compared to a Danish control cohort, these patients were enriched for a subset of rare *RBBP8* variants. Functional

62 analysis revealed that whilst these CtIP variants did not affect DSB resection
63 efficiency, their expression led to deleterious nucleolytic degradation of stalled
64 replication forks in a manner similar to cells lacking BRCA1/BRCA2. Notably,
65 CtIP deficiency promoted the helicase-driven destabilization of RAD51
66 nucleofilaments at damaged replication forks. Taken together, our work
67 identifies CtIP as a critical regulator of replication fork integrity that when
68 mutated may predispose to the development of early-onset breast cancer.
69

Results

Identification of *RBBP8* germline variants. We screened a group of 129 Danish high-risk *BRCA1* and *BRCA2* pathogenic variant-negative breast cancer patients for germline variants in *RBBP8* encoding CtIP (Patient group I, outlined in Supplementary Figure 1). Fifty percent of women had a 1st or 2nd degree relative with breast or ovarian cancer and included women below 35 years of age at the time of diagnosis, male breast cancer patients and six women with early-onset ovarian cancer (Supplementary Table 1). This initial screening identified five different non-synonymous, heterozygous *RBBP8* variants (Table 1 and Figure 1A-B). Three patients were carriers of an in-frame 3-bp deletion in exon 18 (c.2410_2412del; p.E804del), which was detected at an allele frequency of 1.16%. The p.E804del variant is significantly overrepresented in our cohort with respect to 2,000 Danes (12). In addition, two patients were carriers of different missense *RBBP8* variants (c.693T>A, p.S231R in exon 9 and c.1928A>C, p.Q643P in exon 13, respectively), and one patient carried two different missense variants, (c.298C>T, p.R100W in exon 6 and c.2131G>A, p.E711K in exon 15). Only the p.R100W variant was detected in 2,000 Danes, whilst the p.Q643P and the p.E711K variant had not been reported previously (12).

We subsequently sequenced *RBBP8* in a larger series of 1,092 patients negative for *BRCA1* and *BRCA2* pathogenic variants with breast cancer and/or ovarian cancer or other related cancer types, as well as unaffected individuals of families with HBOC (Patient group II, outlined in Supplementary Figure 1). Nine different heterozygous missense variants in *RBBP8* (Table 1 and Figure 1A-B) were identified in 14 females from this cohort. Three patients carried a

p.R110Q variant, two a p.H456R variant, and three carried the p.Q643P variant previously identified among patient group I. A further six variants, p.R502L, p.T675I, p.R805G, p.R839Q, p.P874A and p.E894D, were identified in individual patients. In total, we identified 13 *RBBP8* variants in 21 patients (Table 1), nine of which were observed once. Finally, we explored an international cohort of 1054 breast cancer patients without pathogenic variants in *BRCA1* or *BRCA2* for rare variants in *RBBP8*. Here, we identified 17 different rare variants in 22 patients of which the clinically annotated (n=7) had a median age of 38 at the time of diagnosis (Supplementary Table 2). These *RBBP8*-variants also included the p.Q643P variant and two loss-of-function variants (Supplementary Table 2).

***RBBP8*/CtIP variants display a genome maintenance defect.** Since our genetic screening indicated that *RBBP8* variants could be associated with early-onset breast cancer, we investigated whether they affect known CtIP function(s). Hence, we examined DNA DSB end resection as well as genome stability after exposure to irradiation (IR) or replication stress induced with aphidicolin (APH) or hydroxyurea (HU). To create an isogenic system for our assays, we first depleted endogenous *RBBP8*/CtIP from breast cancer MCF7 cells with siRNA, and complemented cells with re-expression of siRNA-resistant CtIP variants (Figure 2A-B). All variants were well expressed; surprisingly, however, none of these variants affected the ability of cells to perform DNA DSB end resection after irradiation (Figure 2C; Supplementary Figure 2A). The phosphorylation of RPA32 on the S4/S8 residues was used as a readout for the proficiency of DNA DSB end resection after IR in these assays

(13). Next, we monitored genome stability after exposure to IR, APH or HU, using the accumulation of extranuclear micronuclei as a readout (Supplementary Figure 2B). In a manner similar to Wt-CtIP, and in keeping with our findings above, all the tested variants were able to complement the IR-induced genome instability caused by the loss of CtIP (Table 2). Together, these data indicate that the identified germline *RBBP8* variants do not give rise to a detectable impairment of DNA DSB repair. However, expression of several variants (Q643P, E804del, and R805G) as well as the C-terminal truncated CtIP (Δ C) mutant, failed to complement the genome instability induced by APH and HU following depletion of endogenous CtIP (Table 2). This suggests that these variants perturb a function of CtIP specifically associated with the replication stress response. In addition to the Danish breast cancer cohort, we also investigated the *RBBP8* variants present in the international COMPLEXO cohort for genome stability after exposure to APH or HU using variant complementation in CtIP depleted cells. The CtIP-Q643P variant, as well as the truncating variants CtIP-R185* and CtIP-L372* all displayed increased genome instability after replication stress (Supplementary table 3).

CtIP-E804del is proficient in HR repair

To further examine the potential HR repair status of CtIP variants in the Danish breast cancer cohort, we focussed on the CtIP-E804del variant as it was significantly enriched in the cohort. We used the tractable U-2-OS cell line, which is commonly used to evaluate CtIP function (14, 15), and generated an inducible complementation system expressing siRNA resistant GFP-tagged full-length CtIP or the CtIP-E804del variant (Supplementary Figure 2C-H).

Consistent with our previous results in MCF7 cells (Figure 2C), expression of the CtIP-E804del variant in the U-2-OS cells could rescue the DSB resection deficiency resulting from CtIP depletion (Supplementary Figure 2C-D). We then set out to assess HRR efficiency in CtIP-E804del U-2-OS cells, since CtIP-dependent DSB end resection is crucial for efficient HRR. As expected, expression of CtIP-E804del variant could rescue the HRR deficiency caused by CtIP depletion (Supplementary Figure 2E-G). Since HRR deficiency can be therapeutically exploited through the use of PARP inhibitors (PARPi), we also investigated whether CtIP-E804del variant expression promotes PARPi sensitivity. As shown in Supplementary Figure 2H using variant complementation of siRNA depleted cells, CtIP-E804del variant did not display any increase in PARPi sensitivity over and above Wt-CtIP complemented cells. Taken together, these results indicate that the CtIP-E804del variant displays proficient DSB end resection and HRR. Furthermore, this suggests that CtIP variants deficient in responding to replication stress may promote tumorigenesis independently of HRR.

CtIP promotes RAD51 function during replication stress.

In order to functionally characterize a subset of variants in greater detail, the CtIP-Q643P and CtIP-E804del variants were chosen because they were significantly enriched in our Danish breast cancer cohort and were associated with increased genome instability upon HU and APH treatment (Table 2). Additionally, the CtIP-R805G variant was also chosen due to its close amino acid sequence proximity to the CtIP-E804del variant and its defective response to replication stress (Table 2).

170 Notably, Q643P, E804del and R805G CtIP variants could not be linked with
171 deficiency in DNA end resection. As an alternative explanation underlying their
172 functional contribution, we hypothesized that these variants may instead be
173 deficient in replication fork degradation which is a recently emerging role for
174 CtIP (16). To test this hypothesis, we first analyzed the prevalence of RPA foci.
175 This is a robust marker of ssDNA accumulating at replication forks after HU
176 treatment, with both increases and decreases in the number of RPA foci per
177 cell being indicative of replication stress response perturbations. Consistent
178 with previous reports (17), CtIP depletion led to an increase in HU-induced RPA
179 foci formation, which could be rescued by expressing exogenous Wt-CtIP-GFP
180 (Figure 3A-B). Interestingly, this was not the case for both the CtIP-E804del or
181 CtIP-R805G variants (Figure 3A-B). Serving as negative control, variants that
182 did not display genomic instability after replication stress could also rescue the
183 elevated level RPA foci formation resulting from CtIP knockdown
184 (Supplementary Figure 3A). Intriguingly, the CtIP-Q643P variant suppressed
185 RPA in a manner comparable to Wt-CtIP (Figure 3A-B).

186 To obtain insight into the underlying mechanisms, we further examined how
187 CtIP-depleted cells responded to replication stress. Since RAD51
188 nucleofilaments protect stalled replication forks from uncontrolled nucleolytic
189 degradation (5, 18), we addressed whether CtIP affects RAD51 localisation at
190 damaged forks. As shown in Figure 3C-D, HU-induced RAD51 foci formation
191 was reduced in MCF7 cells depleted of CtIP. Notably, neither expression of the
192 E804del nor R805G CtIP variants could complement the loss of HU-induced
193 RAD51 foci formation caused by CtIP depletion (Figure 3C-D and
194 Supplementary Figure 3B), whilst this could be restored by transient expression

of CtIP-Wt and several other CtIP potentially non-pathogenic variants. These data therefore suggest that the Sae2-like domain of CtIP might play a role in recruiting/stabilizing RAD51 after replication stress. Intriguingly, the HU-induced RAD51 response was comparable in cells expressing the CtIP-Q643P variant as to compared to cells expressing Wt-CtIP (Figure 3C-D), which suggests that this variant promotes replication stress-induced genome instability via another mode of action.

In order to directly visualize RAD51 recruitment to the stalled forks after HU treatment, we turned to isolation of proteins on nascent DNA (iPOND), using CLiCK chemistry to conjugate biotin to a nucleoside analog (EdU) incorporated into newly synthesized DNA (19). Our analyses primarily focused on comparing Wt-CtIP with the CtIP-E804del variant, since this variant was the most significantly enriched variant from the Danish cohort that exhibited a defective response to replication stress. In agreement with our previous data (Figure 3C-D), using iPOND, the recruitment of RAD51 to nascent DNA damaged with HU was reduced in the absence of CtIP. Moreover, this deficiency was restored by the complementation with Wt- CtIP. Importantly, however, this was not the case after complementation with the CtIP-E804del mutant (Supplementary Figure 3C). To understand if CtIP is recruited directly to stalled forks after HU treatment, we employed a proximity ligation assay (PLA)-based approach that measures the association of proteins on nascent DNA (20, 21). Following the depletion of CtIP from U-2-OS cells, the expression of Wt-CtIP or CtIP-E804del was induced in cells with doxycycline. Cells were then labeled with EdU for 10 min prior to treatment with 4 mM HU for 5 h. Click

chemistry was then used to conjugate Biotin to EdU and PLA was conducted to detect protein binding to biotin-labeled nascent DNA. Using this approach, our data revealed that Wt-CtIP is present at nascent DNA after replication stress, while CtIP-E804del was absent under the same conditions (Supplementary Figure 3D-E).

Together, these data suggest that CtIP prevents the accumulation of ssDNA at damaged replication forks by recruiting/stabilizing RAD51 and that the cancer-associated CtIP variant E804del compromises this function.

CtIP antagonizes excessive degradation of stalled replication forks through FBH1. Since RAD51 is known to protect stalled replication forks from degradation and loss of CtIP is causing a decrease in RAD51 foci formation, we sought to measure replication fork degradation directly, using the single molecule DNA fibre-based assay (18, 22). CtIP was depleted from U-2-OS cells and expression of Wt-CtIP, the E804del or ΔC variants were induced. These cells were then sequentially pulse-labelled with CldU and IdU to label nascent DNA before prolonged fork stalling with HU (Figure 4A). In keeping with previous reports (23), these analyses showed that loss of CtIP results in increased degradation of nascent DNA at stalled replication forks (Figure 4B). Moreover, this was abolished upon the expression of Wt-CtIP, but not by expression of the ΔC mutant (Figure 4C). Importantly, the E804del variant was partially deficient in replication fork protection after HU (Figure 4C). Thus, we surmise that the role of CtIP in preventing nascent DNA degradation at stalled forks involves its C-terminal Sae2-like domain.

Finally, we asked whether CtIP plays a role in recruiting RAD51 to stalled forks in a manner similar to BRCA1/2 or stabilizing RAD51 at these structures like BOD1L and WRNIP1. Unlike BRCA1/2, BOD1L and WRNIP1 protect damaged forks by suppressing the anti-recombinase activity of proteins such as FBH1 and BLM (15, 20). Moreover, it has been shown that loss of the anti-recombinase FBH1 increases RAD51 foci formation at stalled replication forks (24). Therefore, we hypothesized that FBH1 might be involved in evicting RAD51 from stalled forks in the absence of CtIP. In keeping with this prediction, concomitant depletion of FBH1 and CtIP rescued RAD51 accumulation in HU-treated conditions to control levels (Figure 4D-E). To further explore the link between CtIP and FBH1, we performed fork degradation assays in HU-treated cells depleted of CtIP, FBH1 or CtIP/FBH1 together (Figure 4F). These experiments revealed that loss of FBH1 restored nascent DNA stability in the absence of CtIP (Figure 4F), suggesting that CtIP stabilises RAD51 nucleofilaments to suppress fork degradation. Depletion of FBH1 in cells expressing the CtIP-E804del variant also restored nascent strand stability, and re-stabilized RAD51 at stalled replication forks (Figure 4G-H, Supplementary Figure 4A-B). These data therefore suggest that CtIP regulates replication fork stability by suppressing FBH1-mediated eviction of RAD51 from stalled forks, and that cancer-associated mutations in the C-terminus of CtIP perturb this vital function (Figure 4H).

Discussion

Our study demonstrates a role for rare *RBBP8* variants in the control of DNA replication fork integrity. Altogether we identified 13 *RBBP8* germline variants in 21 patients, of which the C-terminal E804del variant was observed in three patients. Importantly, we identified 3 *RBBP8* variants that displayed increased genome instability. These variants were located in the C-terminus (E804del and R805G) and LMO4-interacting (Q643P) regions of CtIP. The C-terminus region is crucial for CtIP functions in genome maintenance and consistent with this, localization of RAD51 and RPA to sites of damage was impaired by E804del and R805G variants. Regarding the variant in the LMO4-interacting region (Q643P), although the functional role for this domain is unclear, it is conceivable that the breast cancer risk associated with this variant may relate to the dysregulation of LMO4. However, we were unable to detect a variant-dependent interaction between CtIP and LMO4 (Supplementary Figure 4C). Additional studies of this variant may identify additional roles for CtIP in maintaining genome stability and suppressing cancer susceptibility.

Surprisingly, the subset of CtIP variants promoting genome instability were functionally wildtype for DNA DSB end resection and HRR. Instead, we demonstrate that CtIP protects stalled replication forks against enhanced fork degradation by promoting RAD51 nucleofilament stability, and it is this function that is perturbed by variants associated with early-onset breast cancer. Thus, these results suggest that CtIP insufficiency may predispose to breast cancer by allowing deleterious replication fork degradation (Figure 4I). Interestingly, loss of fork protection is a potential target for cancer therapy, since the ability

of BRCA1/2-deficient cells to acquire drug resistance is intimately linked to fork protection (6).

A pathway protecting stalling DNA forks from degradation was first uncovered in cells with BRCA2 insufficiency, and more recently has been reported in cells lacking critical tumor suppressors known to be involved in regulating HRR, including BRCA1, PALB2, and FANCD2 (6, 18, 21, 25). Our research now links CtIP with these factors that allow stable RAD51 accumulation when forks are challenged. However, unlike BRCA1, BRCA2 and PALB2, we suggest that CtIP belongs to a family of replication fork protection factors, including BOD1L and WRNIP1, that regulate the FBH1 helicase, a RAD51-evicting factor. Thus, in the absence of RAD51-stabilising factors, FBH1 reduces the presence of RAD51 at stalled forks, allowing uncontrolled fork degradation that can trigger genome instability. This is an emerging biological response to fork stalling, and the links with tumorigenesis are only now starting to be dissected. Notably, our functional findings on CtIP are in agreement with recently published data that also identify a role for CtIP in suppressing degradation of stalled replication forks (16). The authors focused on the role of the N-terminal region of CtIP that helps to minimize nucleolytic degradation by the DNA2 nuclease. Thus far, we have not identified cancer-associated disabling variants in this CtIP region.

The roles of CtIP in breast cancer predisposition and progression are not well understood, though studies have indicated that a lack or low levels of CtIP expression in tumor cells is associated with a reduced survival rate (23, 26). Furthermore, tumors lacking CtIP display an impaired ability to repair DSB,

which leads to increased sensitivity to PARP inhibitors (26, 27). Thus, determining the impact of identified variants in CtIP on its function should be considered when trying to personalise a therapeutic approach for treating a specific patient. Intriguingly, analysis of a cohort of 129 *BRCA1* and *BRCA2* mutation-negative Australian breast cancer patients failed to demonstrate an enrichment of coding variants in *RBBP8* (28). In fact, no coding *RBBP8* variants were identified except for a polymorphism in intron 6. In contrast, a recent Spanish study identified two truncating *RBBP8* variants in two early-onset *BRCA1/2* mutation negative BC patients (29). Furthermore, we identified two functionally damaging truncating variants in the COMPLEXO cohort in addition to the Q643P variant also described here. The differences between studies may reflect population differences, cohort sizes as well as age of BC onset in the cohorts.

Murine studies have indicated that CtIP haploinsufficiency is tumor promoting, whereas a complete loss of CtIP is detrimental leading to inviability of mice (30). In contrast, murine tissue-specific conditional CtIP ablation systems indicated that a complete loss of CtIP suppresses tumorigenesis (31). However, it is likely that these observations are due to a deleterious decrease in cellular fitness linked to a complete loss of HRR. Importantly, we have shown that a subset of *RBBP8* variants identified in this study are hypomorphic in a manner where they impair some functions of CtIP but not all. Based on this, we propose that hypomorphic but not loss-of-function mutations in *RBBP8* predispose to early-onset breast cancer. We cannot exclude the possibility that these variants may represent rare variants with little association with cancer development.

342 However, it is noteworthy that we identified *RBBP8* germline variants in early-
343 onset breast cancer patients at a frequency similar to that previously reported
344 for HBOC-associated mutations in *BRIP1*, *RECQL1* and *PALB2* (3, 8-10).
345 Thus, since our data indicates that *RBBP8* variants are more frequent in early-
346 onset breast cancer cases than in unaffected population-matched controls, this
347 warrants consideration of *RBBP8* being included in the gene panel when
348 carrying out breast cancer predisposing sequencing studies. Finally, our study
349 shows the usefulness of combining genetic screening in a high-risk phenotype
350 with comprehensive variant-centered functional analysis to identify and classify
351 new variants implicated in hereditary cancer syndromes.

352

Experimental procedures

Patients

All patient samples were consecutively recieved for HBOC diagnostics over a period of 20 years, according to the contempary national HBOC guidelines (Danish Breast Cancer Cooperative Group (DBCG)). Clinical and histopathological data were retrieved from the Danish Pathology Registry and the DBCG registry. Patients were diagnosed between year 1978 to 2016.

Patient group I included 129 breast and/or ovarian cancer patients, previously identified as *BRCA1/2* pathogenic-variant-negative as part of their diagnostic work-up (124 females and 5 males). Female patients diagnosed with ovarian or with breast cancer at the age of 35 years or younger, while male breast cancer patients were included regardless of age at time of diagnosis. Among the female patients, 116 had breast cancer only, six had ovarian cancer only, one had breast and ovarian cancer, and one had breast and cervical cancer. Four of the men had breast cancer only, whereas 1 had both breast and prostate cancer. Mean age at time of diagnosis of the female patients was 30 years and for male 59 years.

Patient group II included 1,092 *BRCA1/2* - negative samples from unselected and consecutive patients undergoing genetic screening for HBOC according to clinical guidelines as described above.

Sequencing of *RBBP8* in patient group I

Genomic DNA was purified from peripheral blood samples and library preparation was performed using SeqCap EZ Human Exome Library v3 (Roche NimbleGen, Madison, WI, USA) or SureSelect All Exon kit v5 (Agilent Technologies, Santa Clara, CA, USA) following manufactures' instructions. Sequencing was conducted using the HiSeq2500 or NextSeq500 platforms from Illumina (San Diego, Ca, USA). The average coverage of all exomes was 65x.

Data processing

Fastq files were processed using CLC Biomedical Genomics Workbench v3 (Qiagen, Hilden, Germany). Reads were mapped to the human reference genome hg19/GRCh37 and variant calling was performed by a Maximum Likelihood approach on a Bayesian model. Variants were called with a minimum of 10 reads, 3 counts and a frequency of >25 %. Called variants were filtered using Ingenuity Variant Analysis (<http://ingenuity.com>). First, variants with call quality <20 and read depth <10; were disregarded. Second, variants with an allele frequency >1% of the public variant database including 1000 genomes project (www.1000genomes.org), ExAC (<http://exac.broadinstitute.org>) or gnomAD (<http://gnomad.broadinstitute.org>), or unless established as a pathogenic common variant, were excluded. Third, only coding non-synonymous variants and splice-site variants (+/-2bp) were kept. Finally, output was filtered to include the *RBBP8* gene. Samples (n=1054) from the COMPLEXO consortium were initially processed from raw fastq reads and aligned to the human genome reference (hg19) using bwa (v0.5.9) on a per lane basis. Alignment file pre-processing and germline variant calling was

performed by The Genome Analysis Toolkit (GATK) v3.1 (v3.1-144).
HaplotypeCaller algorithm was used to generate variant files (.vcf) which were
filtered to include only rare variants in the *RBBP8* gene (<1% in ExAC).

Sequencing of *RBBP8* in Patient group II

Screening of the larger group for *RBBP8* variants was performed using a gene
panel. The library was designed to capture all exons as well as the first and last
50 bp of the intronic regions. Samples were pooled into groups of four and
deeply sequenced (average coverage of 5.500x). Mapping and variant calling
was done as described for patient group I, however as samples were pooled
into groups of four, variants were called with a minimum of 100 reads, 10 counts
and frequency of 6.25 % (corresponding to a variant detection rate of 25 % pr.
sample). Variant filtering was performed using Ingenuity Variant Analysis.

Sanger sequencing

All non-polymorphic *RBBP8* variants identified by sequencing of the two patient
groups were verified by PCR and Sanger sequencing (for primer sequences
see Supplemental table 4).

Statistical Analysis of allelic association with Breast Cancer

Fisher's exact test was employed to determine if identified *RBBP8* variants
were enriched in the examined breast cancer patient cohorts compared to the
2,000 Danes were used as controls in the statistical analysis.

Cell culture

The human cancer cell lines were cultured for 5 days at 37°C and 5% CO₂ as follows: The human breast cancer cells (MCF7) were cultured in RPMI (GIBCO, Life Technologies), supplemented with 10% FBS (Sigma Aldrich), and 1% penicillin/streptomycin (GIBCO, Life Technologies). The human osteosarcoma cell line (U-2-OS), harboring inducible GFP-tagged siRNA resistant CtIP were grown in Dulbecco's modified Eagle's medium with 10% tetracycline-free FBS (Clontech) 1% penicillin/streptomycin (GIBCO, Life Technologies), 100 ug/ml Zeocin (Invitrogen) and 5 ug/ml Blasticidin (Invitrogen). The human embryonic kidney 293FT cells were grown in Dulbecco's modified Eagle's medium with 10% FBS (Sigma Aldrich) and 1% penicillin/streptomycin (GIBCO, Life Technologies).

Lentiviral infection

The doxycycline inducible stable U-2-OS cell lines expressing the pcDNA4/TO tagged siRNA-resistant versions of wild-type and mutant CtIP were established by cloning CtIP cDNA into pcDNA4/TO-GFP vector (Invitrogen). The ΔC truncation of CtIP is lacking amino acids 790–897.

The GFP-CtIP plasmids were sub-cloned into pLVX-TetOne Vector (Clontech) and were co-transfected with Pax8 (Clontech) and VSVG (Clontech) into HEK293 FT cells using EugeneHD (Promega). The generated CtIP lentivirus were then transduced into U-2-OS using polybrene according to the manufacturer's protocol resulting in cell lines expressing GFP- tagged siRNA-resistant CtIP Wt, E804del, or ΔC in a Tet-on system. To induce expression of siRNA resistant CtIP, doxycycline (1 ng/ml) was added to the medium for approximately 24 h.

452

453 **Site directed mutagenesis**

454 The mutant CtIP plasmids were generated by site-directed mutagenesis of the
455 siRNA-resistant Wt-CtIP. The following primers were used:

456 CtIP R100W: Fw: 5'-ACTGAAGAACATATGTGGAAAAACAGCAAG

457 CtIP R100W: Re: 5'-CTTGCTGTTTTTCCACATATGTTCTTCAGT

458 CtIP R110Q: Fw: 5'-GAGTTTGAAAATATCCAGCAGCAGAATCTTAAA

459 CtIP R110Q: Re: 5'-TTTAAGATTCTGCTGCTGGATATTTTCAAACCTC

460 CtIP R185*: Fw: 5'-AGAACCCCCATGTCTGATACATAGAACAAA

461 CtIP R185*: Re: 5'-TTTGTCTCTATGTATCAGACATGGGGGTTCT

462 CtIP V198M: Fw: 5'-AAATTGGAGCACTCTATGTGTGCAAATGAAAT

463 CtIP V198M: Re: 5'-ATTTCAATTTGCACACATAGAGTGCTCCAATTT

464 CtIP S231R: Fw: 5'-CACTTATGACCAAAGACAATCTCCAATGGCC

465 CtIP S231R: Rev: 5'-GGCCATTGGAGATTGTCTTTGGTCATAAGTG

466 CtIP E267G: Fw: 5'-ACTTGGTGTTC AAGGAGAATCTGAAACTC

467 CtIP E267G: Re: 5'-GAGTTTCAGATTCTCCTTGAACACCAAGT

468 CtIP Q272E: Fw: 5'-AAGAATCTGAAACTGAAGGTCCCATGAG

469 CtIP Q272E: Re: 5'-CTCATGGGACCTTCAGTTTCAGATTCTT

470 CtIP G331A: Fw: 5'-ATCTCCTGTATTTGCAGCTACCTCTAGTA

471 CtIP G331A: Re: 5'-TACTAGAGGTAGCTGCAAATACAGGAGAT

472 CtIP Q352P: Fw: 5'-CCTTCTCTTTTACCGCCTGGGAAAAAAA

473 CtIP Q352P: Re: 5'-TTTTTTTCCCAGGCGGTAAAAGAGAAGG

474 CtIP I369V: Fw: 5'-CTTTTAGCAACACTTGTGTATCTAGATTAGAAAA

475 CtIP I369V: Re: 5'-TTTTCTAATCTAGATACACAAGTGTTGCTAAAAG

476 CtIP L372*: Fw: 5'-CACTTGTATATCTAGATGAGAAAAAACTAGATCA

477 CtIP L372*: Re: 5'-TGATCTAGTTTTTTCTCATCTAGATATACAAGTG
 478 CtIP E414D: Fw: 5'-AATAAAAATATAAGTGATTCCCTAGGTGAACAGA
 479 CtIP E414D: Re: 5'-TCTGTTACCTAGGGAATCACTTATATTTTTATT
 480 CtIP H456R: Fw: 5'-GAGGAAGAAAGTGAACGTGAAGTAAGCTGC
 481 CtIP H456R: Re: 5'-GCAGCTTACTTCACGTTCACCTTCCTC
 482 CtIP R502L: Fw: 5'-TTTTCAGCTATTCAGCTTCAAGAGAAAAGCCAA
 483 CtIP R502L: Re: 5'-TTGGCTTTTCTCTTGAAGCTGAATAGCTGAAAA
 484 CtIP E552D: Fw: 5'-ATTCCCCAGGGGATCCCTGTTTACA
 485 CtIP E552D: Re: 5'-TGTGAACAGGGATCCCCTGGGGAAT
 486 CtIP R589H: Fw: 5'-TTTAAAATTCCTCTACATCCACGTGAAAGTTTG
 487 CtIP R589H: Re: 5'-CAAACCTTTCACGTGGATGTAGAGGAATTTTAAA
 488 CtIP Q643P: Fw: 5'-AAAATAAAGTCTCTACCAAACAACCAAGATGTA
 489 CtIP Q643P: Re: 5'-TACATCTTGGTTGTTTGGTAGAGACTTTATTTT
 490 CtIP E711K : Fw: 5'-CAAGAGCAGAAGGGAAAAAAAAGTTCAAATG
 491 CtIP E711K : Re: 5'-CATTTGAACTTTTTTTTCCCTTCTGCTCTTG
 492 CtIP E716K: Fw: 5'-GGGAGAAAAAAGTTCAAATAAAGAAAGAAAAATGAA
 493 TG
 494 CtIP E716K: Re: 5'-CATTCATTTTCTTTCTTTATTTGAACTTTTTTCTCCC
 495 CtIP E804del: Fw: 5'-GTGGTTCGGAAAAAAGAGAGAAGA...CAG
 496 CtIP E804del : Re: 5'-GTGTGCCCAAGCAGTTTTCTTCTC...CAC
 497 CtIP R805: Fw: 5'-GTTCGGAAAAAAGAGGAGGGAAGAAAAGCTGCTTGGGC
 498 CtIP R805G : Re: 5'-GCCCAAGCAGTTTTCTTCCCTCTTTTTTCCGAA
 499 CtIP R839G : Fw: 5'-GGAATGTAGCGGAATCCGTGTCTTGAGCAGGAA
 500 CtIP R839G : Re: 5'-TTCCTGCTCAAGACACGGATTCCGCTACATTCC
 501 CtIP P847A : Fw: 5'- AAGGAAGATCTTGATGCTTGTCTCGTCCAA

502 CtIP P847A : Re: 5'- TTGGACGAGGACAAGCATCAAGATCTTCCTT
503 CtIP R877H: Fw: 5'-TTGATCCTTGTCTCATCCAAAAAGACGT
504 CtIP R877H: Re: 5'-ACGTCTTTTTGGATGAGGACAAGGATCAA
505 CtIP E894D : Fw: 5'- TCCAAAAGGCAAGGACCAGAAGACATAGACG
506 CtIP E894D : Re: 5'- CGTCTATGTCTTCTGGTCCTTGCCTTTTGA
507 CtIP ΔC: Fw: 5'-GAAAGAGAGACTAGCTAGCAAAATTTTCCTCAT
508 CtIP ΔC: Re: 5'-ATGAGGAAAATTTTGCTAGCTAGTCTCTCTTTC

509 The PFU ultra-high-fidelity polymerase (Agilent) was used according to the
510 manufacturer's protocol.

511

512 **Oligonucleotides and transfection**

513 For siRNA transfections (48 h), Lipofectamine RNAiMAX (Invitrogen) was used
514 according to the manufacturer's protocol. MISSION® siRNA universal negative
515 control (UNC, Sigma) was used as a negative control, and the oligonucleotide
516 sequences used for knockdown of CtIP was 5'-GCUAAAACAGGAACGAAU
517 which was obtained from Microsynth (Balgach,Switzerland), for depleting
518 FBH1, a mix of two sequences 5'-GGGAUGUUCUUUUGAUAAA and 5'-
519 CCAUCCAACUUACACAUGA was used.

520

521 **Reagents**

522 Hydroxyurea (Sigma aldrich) was used at a final concentration of 4 mM for the
523 indicated time. Aphidicolin (Sigma aldrich) was used at a final concentration of
524 0.3 μM for the indicated time. Furthermore, Cytochalasin B (Sigma aldrich) was
525 used at a concentration of 1 μg/ml.

526

Western blotting and antibodies

Cells were lysed on ice in EBC buffer (50 mM Tris, pH 7.4, 120 mM NaCl, 0.5% NP-40, and 1 mM EDTA) containing protease inhibitors (1% vol/vol aprotinin, 5 µg/ml leupeptin, 1 mM PMSF), phosphatase inhibitors (1 mM NaF, 10 mM β-glycerophosphate), and 1 mM DTT. The lysates were sonicated, using a digital sonifier (102C CE Converter; Branson), followed by centrifugation at 20,000xg for 15 min. Proteins were resolved by SDS-PAGE and transferred to nitrocellulose membrane. The membrane were incubated with primary antibody followed by incubation with secondary antibody (HRP-conjugated anti-mouse or -rabbit IgG; Vector Laboratories). Immunoblots were performed using the following antibodies: CtIP (#A300488A, Bethyl Laboratories), RAD51 (#8349, Santa Cruz), RAD51 (#63801, Abcam), PCNA (#18197, Abcam), FBH1 (FBXO18, #81563, Santa Cruz), GFP (#1181446000, Roche), Actin (#AB1501; Millipore), RPA2 S4/8 (#A300245A, Biosite), RPA (#NA29L, Millipore), Vinculin (#V9131, Sigma), BRCA2 (#OP95, Calbiochem), H3 (#1791, Abcam), HA (#MMS-101P-500, Covance).

Immunofluorescence

The cells were grown on coverslips and treated as indicated and then prepared for immunofluorescence staining. Primary antibodies used were RAD51 (1:1,000, 70-001, BioAcademia Jpn), GFP (1:1,000, #1181446000, Roche), RPA (#NA29L, Millipore), RPA2 S4/8 (#A300245A, Biosite). Anti-rabbit Alexa Fluor 647, anti-mouse Alexa Fluor 488 (1:2,000, A21245, A11017, Life Technologies) were used as secondary antibodies. For RAD51, immunofluorescence cells were pre-extracted twice for 3 min in CSK buffer

(0.5% Triton X-100, 20 mM Hepes pH 7.4, 100 mM NaCl, 3 mM MgCl₂, and 300 mM sucrose) followed by fixation in 4% paraformaldehyde (PFA) (VWR). Cells were permeabilized in 0.5% Triton X-100 followed by incubation in blocking buffer (1% BSA, 0.15% glycine, 0.1% Triton X-100 in PBS wash buffer (1x PBS, 0.1% Tween-20, 1 mM CaCl₂, 0.5 mM MgCl₂). Primary antibody was incubated for 1 h at room temperature in blocking buffer, followed by three washes with PBS wash buffer. Secondary antibody was incubated for an additional hour, washed 3x with PBS wash buffer, and mounted in mounting vectashield with diamidino-2-phenylindole (DAPI) (vector Laboratories). EdU staining was done per manufacturer's instructions (Life Technologies). Z-stack images were acquired on a confocal Zeiss LSM 510 meta microscope workstation, and images were processed and foci enumerated using Fiji (ImageJ).

Micronuclei assay

Cells were cultured on coverslips post-transfection and were incubated for another 24 h before starting the treatment of the cells. Cells were treated with Aphidicolin (Sigma aldrich) for 16 h or Hydroxyurea (Sigma Aldrich) for 5 h. In addition, cells were treated with Cytochalasin B (Sigma Aldrich) for 36 h (MCF7), to inhibit cytokinesis, and then fixed in 4% paraformaldehyde (PFA) (VWR). Next, the cells were permeabilized with 0.25% Triton X-100 solution, washed twice with 1xPBS and mounted in Vectashield with diamidino-2-phenylindole (DAPI) (vector Laboratories), binucleated cells with a micronuclei was counted manually using a confocal Zeiss LSM 510 meta microscope and a Scan^R workstation (Olympus).

577

578 **HR assay**

579 U-2-OS cells transfected with CtIP siRNA followed by transfection of gRNAs
580 targeting the LMNA locus and the Ruby Donor plasmid as described in
581 reference (32) together with empty vector or siRNA-resistant Wt, E804del or
582 Δ C CtIP. After 48 h, Lamin A (LMNA) genes were monitored by microscopy.

583

584 **iPond**

585 DOX-inducible U-2-OS cells were transfected with both UNC (negative control)
586 or CtIP siRNA and 24 h later, cells were induced with DOX for 24 h. Cells were
587 incubated with 10 μ M EdU for 15 min, washed in media, then incubated with
588 media containing 4 mM HU for 5 h, cross-linked with 1% formaldehyde,
589 harvested and permeabilised. Biotin azide was covalently attached to EdU
590 within newly replicated DNA using a Click reaction, and EdU containing DNA
591 was precipitated using Streptavidin agarose beads. Eluted proteins were then
592 analysed by SDS-PAGE and WB.

593

594 **DNA fibres**

595 DNA fibres were carried out as described previously (22). Twenty-four hours
596 post siRNA transfection cells were treated with doxycycline to induce CtIP
597 expression, and left for a further 24 h. Cells were then pulse-labelled with CldU
598 and IdU for 20 min each before a 5 h exposure to 4 mM HU. At least 200
599 replication forks were analysed per condition. Tract lengths were measured
600 using Fiji, and ratios calculated.

601

Proximity ligation assay on nascent DNA

Twenty-four hours post siRNA transfection cells were treated with doxycycline to induce CtIP expression, and left for a further 24 h. Cells were then pulse-labelled with 10 mM EdU for 10 min followed by 4 mM HU for 5 hr. After the indicated treatment, cells were pre-extracted for 5 min in buffer (0.5% Triton X-100, 10 mM PIPES pH 6.8, 20 mM NaCl, 3 mM MgCl₂, and 300 mM sucrose) followed by fixation in 4% paraformaldehyde (PFA) (VWR). Cells were incubated in blocking buffer (3% BSA, in PBS with 0.1% Na Azide for 1hr room temperature or O/N in the cold room). After blocking, cells were subjected to Click reaction with biotin-azide for 30 min and incubated overnight with the two relevant primary antibodies at 4°C. The primary antibodies were diluted in PBS with 3% FCS. The primary antibodies used were rabbit polyclonal anti-biotin (1:500, #A150-109A, Bethyl), mouse monoclonal anti-biotin (1:500, #200-002-211, Jackson immunoresearch), rabbit polyclonal anti-CtIP (1:500, # A300-266A, Bethyl). The PLA reaction (Duolink, Sigma Aldrich) to detect anti-biotin antibodies used were performed according to manufacturer instructions.

Immunoprecipitation

Extracts for immunoprecipitation were prepared using immunoprecipitation buffer (50 mM Hepes, pH 7.5, 150 mM NaCl, 1 mM EDTA, 2.5 mM EGTA, 10% glycerol, 0.1% Tween) with protease inhibitors. Following preclearing with IgG-coupled protein G beads (GE Healthcare), the lysates were incubated with monoclonal anti-HA (Covance), and complexes were captured using Protein G Sepharose beads (GE Healthcare) for at 4°C on a rotator. The beads were washed five times followed by elution of bound proteins in Laemmli sample

buffer.

PARPi sensitivity Assay

DOX-inducible U-2-OS cells were seeded on to the CellCarrier-384 Ultra Microplates (PerkinElmer, Massachusetts, United States) and reverse transfection was performed using Lipofectamine RNAiMAX as per the manufacturer's recommendation. After 24 h, DMSO and different concentrations of Talazoparib (BMN 673, Axon Medchem, the Netherlands) were added to the respective wells. On day 3, DMSO and PARPi containing media were replenished. At day 5, CellTiter-Glo (Promega, Wisconsin, United States) was used to quantify the number of viable cells as per the manufacturer's recommendation. Surviving fractions were calculated relative to DMSO-exposed cells for each PARPi concentration.

Statistics

Normal distribution was assessed for all experiment. Micronuclei data was normally distributed and subsequently analyzed using a One-way ANOVA and Dunnett's multiple comparison testing, comparing all variants to Wt-CtIP-GFP. The PARP inhibitor data (Supplementary Figure 2i) were Johnson transformed and the obtained, normally distributed data were fitted with a linear mixed model, with replicates as random effect. Multiple comparisons were performed with the lsmeans/diffmeans and the contrast function of the lmer package in R. Significant codes shown are comparing siCtIP and siBRCA2 to the negative control (siUNC). Foci counts, immunofluorescence intensities as well as HRR data were not normally distributed. Therefore, ranks were assigned to all data

from three biologically independent replicates, based on the number of foci/
immunofluorescence intensity. The obtained ranks were used to fit a linear
mixed model. *P* values were adjusted using the holm method if more than two
comparisons were made. Biologically relevant *p* values are reported with the
following significant codes: $p < 0.0001$ '***'; $p < 0.001$ '**'; $p < 0.05$ '*'. All graphs
represent the mean (red line) \pm SEM (black).

Study approval

The study was approved by The Capital Region of Denmark (H-4-2010-050)
and The Danish data Protection Agency (RH-2016-353, I-Suite no.: 05097)
and DBCG (jr. no.: DBCG-2013-15).

Author Contributions

R.Z. designed and performed the cell biology experiments and iPOND experiment. M.R.H. designed and performed DNA fibre assay. K.V. performed Micronuclei and HRR assays. B.E. diagnosed and enrolled the breast cancer patients. M.R., B.B. and F.C.N performed sequencing and data analysis. A.N.K. generated an inducible complementation system in U-2-OS cells. H.R. designed the cell biology experiments. M.B. performed the PARPi experiments. R.Z, B.B., M.R.H., M.R., F.C.N., G.S.S. and C.S.S wrote the manuscript. The study was planned and supervised by G.S.S., F.C.N. and C.S.S.

Acknowledgements

We thank the Complexo network for data access and advice, see supplementary acknowledgments for consortium details. Claus S. Sørensen is funded by the Danish Cancer Society, the Danish Medical Research Council, and The Lundbeck Foundation. Martin R. Higgs is funded by an MRC Career Development Fellowship (MR/P009085/1) and a Birmingham Fellowship awarded by the University of Birmingham. Grant S. Stewart is funded by a CR-UK Programme Grant (C17183/A23303). FCN is funded by The Lundbeck Foundation and The Research Council of The Capital Region of Denmark. COMPLEXO is support by a program grant from the National Health and Medical Research Council of Australia (APP1074383). We thank Alex Sartori (University of Zurich) for sharing unpublished data with us.

References

1. Nielsen FC, van Overeem Hansen T, and Sorensen CS. Hereditary breast and ovarian cancer: new genes in confined pathways. *Nat Rev Cancer*. 2016;16(9):599-612.
2. Sun J, et al. Mutations in RECQL Gene Are Associated with Predisposition to Breast Cancer. *Plos Genetics*. 2015;11(5).
3. Cybulski C, et al. Germline RECQL mutations are associated with breast cancer susceptibility. *Nature Genetics*. 2015;47(6):643-6.
4. Santos-Pereira JM, and Aguilera A. R loops: new modulators of genome dynamics and function. *Nat Rev Genet*. 2015;16(10):583-97.
5. Schlacher K, Christ N, Siaud N, Egashira A, Wu H, and Jasin M. Double-strand break repair-independent role for BRCA2 in blocking stalled replication fork degradation by MRE11. *Cell*. 2011;145(4):529-42.
6. Chaudhuri AR, et al. Replication fork stability confers chemoresistance in BRCA-deficient cells (vol 535, pg 382, 2016). *Nature*. 2016;539(7629):456-.
7. Couch FJ, Nathanson KL, and Offit K. Two decades after BRCA: setting paradigms in personalized cancer care and prevention. *Science*. 2014;343(6178):1466-70.
8. Foo TK, et al. Compromised BRCA1-PALB2 interaction is associated with breast cancer risk. *Oncogene*. 2017;36(29):4161-70.

- 713 9. Seal S, et al. Truncating mutations in the Fanconi anemia J gene
714 BRIP1 are low-penetrance breast cancer susceptibility alleles. *Nat*
715 *Genet.* 2006;38(11):1239-41.
- 716 10. Rahman N, et al. PALB2, which encodes a BRCA2-interacting protein,
717 is a breast cancer susceptibility gene. *Nat Genet.* 2007;39(2):165-7.
- 718 11. Golmard L, et al. Germline mutation in the RAD51B gene confers
719 predisposition to breast cancer. *BMC Cancer.* 2013;13:484.
- 720 12. Lohmueller KE, et al. Whole-exome sequencing of 2,000 Danish
721 individuals and the role of rare coding variants in type 2 diabetes. *Am J*
722 *Hum Genet.* 2013;93(6):1072-86.
- 723 13. Bunting SF, et al. 53BP1 inhibits homologous recombination in Brca1-
724 deficient cells by blocking resection of DNA breaks. *Cell.*
725 2010;141(2):243-54.
- 726 14. Gossen M, and Bujard H. Tight control of gene expression in
727 mammalian cells by tetracycline-responsive promoters. *Proc Natl Acad*
728 *Sci U S A.* 1992;89(12):5547-51.
- 729 15. Sartori AA, et al. Human CtIP promotes DNA end resection. *Nature.*
730 2007;450(7169):509-14.
- 731 16. Przetocka S, et al. CtIP-Mediated Fork Protection Synergizes with
732 BRCA1 to Suppress Genomic Instability upon DNA Replication Stress.
733 *Mol Cell.* 2018;72(3):568-82 e6.
- 734 17. Raderschall E, Golub EI, and Haaf T. Nuclear foci of mammalian
735 recombination proteins are located at single-stranded DNA regions
736 formed after DNA damage. *Proc Natl Acad Sci U S A.*
737 1999;96(5):1921-6.

- 738 18. Schlacher K, Wu H, and Jasin M. A distinct replication fork protection
739 pathway connects Fanconi anemia tumor suppressors to RAD51-
740 BRCA1/2. *Cancer Cell*. 2012;22(1):106-16.
- 741 19. Sirbu BM, Couch FB, and Cortez D. Monitoring the spatiotemporal
742 dynamics of proteins at replication forks and in assembled chromatin
743 using isolation of proteins on nascent DNA. *Nat Protoc*. 2012;7(3):594-
744 605.
- 745 20. Petruk S, et al. TrxG and PcG proteins but not methylated histones
746 remain associated with DNA through replication. *Cell*. 2012;150(5):922-
747 33.
- 748 21. Taglialatela A, et al. Restoration of Replication Fork Stability in BRCA1-
749 and BRCA2-Deficient Cells by Inactivation of SNF2-Family Fork
750 Remodelers. *Mol Cell*. 2017;68(2):414-30 e8.
- 751 22. Higgs MR, et al. BOD1L Is Required to Suppress Deleterious
752 Resection of Stressed Replication Forks. *Mol Cell*. 2015;59(3):462-77.
- 753 23. Soria-Bretones I, Saez C, Ruiz-Borrego M, Japon MA, and Huertas P.
754 Prognostic value of CtIP/RBBP8 expression in breast cancer. *Cancer*
755 *Med*. 2013;2(6):774-83.
- 756 24. Simandlova J, et al. FBH1 helicase disrupts RAD51 filaments in vitro
757 and modulates homologous recombination in mammalian cells. *J Biol*
758 *Chem*. 2013;288(47):34168-80.
- 759 25. Higgs MR, et al. Histone Methylation by SETD1A Protects Nascent
760 DNA through the Nucleosome Chaperone Activity of FANCD2. *Mol*
761 *Cell*. 2018;71(1):25-41 e6.

- 762 26. Wang J, Ding Q, Fujimori H, Motegi A, Miki Y, and Masutani M. Loss of
763 CtIP disturbs homologous recombination repair and sensitizes breast
764 cancer cells to PARP inhibitors. *Oncotarget*. 2016;7(7):7701-14.
- 765 27. Lin ZP, Ratner ES, Whicker ME, Lee Y, and Sartorelli AC. Triapine
766 disrupts CtIP-mediated homologous recombination repair and
767 sensitizes ovarian cancer cells to PARP and topoisomerase inhibitors.
768 *Mol Cancer Res*. 2014;12(3):381-93.
- 769 28. Gorringe KL, Choong DY, Lindeman GJ, Visvader JE, and Campbell
770 IG. Breast cancer risk and the BRCA1 interacting protein CTIP. *Breast
771 Cancer Res Treat*. 2008;112(2):351-2.
- 772 29. Bonache S, et al. Multigene panel testing beyond BRCA1/2 in
773 breast/ovarian cancer Spanish families and clinical actionability of
774 findings. *J Cancer Res Clin Oncol*. 2018;144(12):2495-513.
- 775 30. Chen PL, et al. Inactivation of CtIP leads to early embryonic lethality
776 mediated by G1 restraint and to tumorigenesis by haploid insufficiency.
777 *Mol Cell Biol*. 2005;25(9):3535-42.
- 778 31. Reczek CR, Shakya R, Miteva Y, Szabolcs M, Ludwig T, and Baer R.
779 The DNA resection protein CtIP promotes mammary tumorigenesis.
780 *Oncotarget*. 2016;7(22):32172-83.
- 781 32. Pinder J, Salsman J, and Dellaire G. Nuclear domain 'knock-in' screen
782 for the evaluation and identification of small molecule enhancers of
783 CRISPR-based genome editing. *Nucleic Acids Res*. 2015;43(19):9379-
784 92.
- 785

849 Tables

850 Table 1. Identified *RBBP8* variants and allele frequencies. AF = Allele
851 Frequency; Fisher Exact Test for AF in Group I and Group I + II compared to
852 AF in controls (2.000 Danish individuals (Lohmueller et al., 2013)). Non-Finnish
853 European (NFE) in gnomAD.

Nucleotide (HGVS)	Protein (HGVS)	Exon	Group I	Group II	AF Group I (%)	AF Group I + II (%)	AF controls (%)	AF NFE (%)	p-value AF (Group I vs controls)	p-value AF (Group I + II vs controls)
c.298C>T	p.R100W	6	1		0.388	0.041	0.025	0.008	ns	ns
c.329G>A	p.R110Q	6		3	-	0.123	0.153	0.070	-	ns
c.693T>A	p.S231R	9	1		0.388	0.041	-	-	ns	ns
c.1367A>G	p.H456R	12		2	-	0.082	0.127	0.220	-	ns
c.1505G>T	p.R502L	12		1	-	0.041	0.025	0.003	-	ns
c.1928A>C	p.Q643P	13	1	3	0.388	0.164	-	0.014	ns	0.02
c.2024C>T	p.T675I	14		1	-	0.041	-	0.011	-	ns
c.2131G>A	p.E711K	15	1		0.388	0.041	-	-	ns	ns
c.2410_2412del	p.E804del	18	3		1.163	0.123	-	0.015	0.0002	ns
c.2413A>G	p.R805G	18		1	-	0.041	-	0.003	-	ns
c.2516G>A	p.R839Q	19		1	-	0.041	-	0.088	-	ns
c.2620C>G	p.P874A	20		1	-	0.041	-	0.008	-	ns
c.2682G>C	p.E894D	20		1	-	0.041	-	-	-	ns

854
855
856
857
858
859
860
861
862
863
864
865

Table 2. CtIP suppresses genomic instability at perturbed replication forks. MCF7 cells transfected with the indicated siRNA followed by transfection of Wt or its mutated CtIP variants. Further, cells were treated with IR or the indicated dose of APH for 16 h or 4mM HU for 5h and Cytochalasin B for 36 h. DAPI stain was used to visualize nuclei. Cells were imaged with a 20x objective on a Scan^R workstation (Olympus). At least 100 green cells were counted for each genotype per experiment. One-Way ANOVA with Dunnett's multiple comparison test was performed on three independent replicates. All variants were compared to Wt-CtIP-GFP.

CtIP variants	Cytochalasin B		IR		APH		HU	
	% of binuclei with micronuclei	p value	% of binuclei with micronuclei	p value	% of binuclei with micronuclei	p value	% of binuclei with micronuclei	p value
Vector (GFP)	49.95		67.30		66.67		67.14	
Wt	47.37	-	46.46	-	47.96	-	48.36	-
R1100W	45.13	Ns	48.38	ns	47.53	Ns	47.39	ns
R110Q	46.46	Ns	47.99	ns	49.31	Ns	50.18	ns
S231R	47.09	Ns	48.29	ns	49.29	Ns	47.36	ns
H456R	47.76	Ns	49.76	ns	47.99	Ns	45.34	ns
R502L	48.77	Ns	49.43	ns	50.12	Ns	50.14	ns
R589H	48.99	Ns	48.04	ns	48.77	Ns	47.70	ns
Q643P	49.33	Ns	48.45	ns	60.74	**** (0.0001)	57.83	** (0.0030)
E711K	46.35	Ns	48.03	ns	45.47	Ns	48.20	ns
E804del	49.34	Ns	47.99	ns	65.32	**** (0.0001)	69.32	**** (0.0001)
R805G	51.62	Ns	48.94	ns	66.67	**** (0.0001)	68.15	**** (0.0001)
R839Q	49.79	Ns	47.60	ns	49.12	Ns	48.28	ns
P874A	48.72	Ns	48.89	ns	50.20	Ns	48.53	ns
E894D	47.46	Ns	47.39	ns	49.09	Ns	49.17	ns
delta C	50.37	Ns	61.26	**** (0.0001)	59.38	*** (0.0002)	58.78	*** (0.0010)

Figure 1 Identification of *RBBP8* germline variants

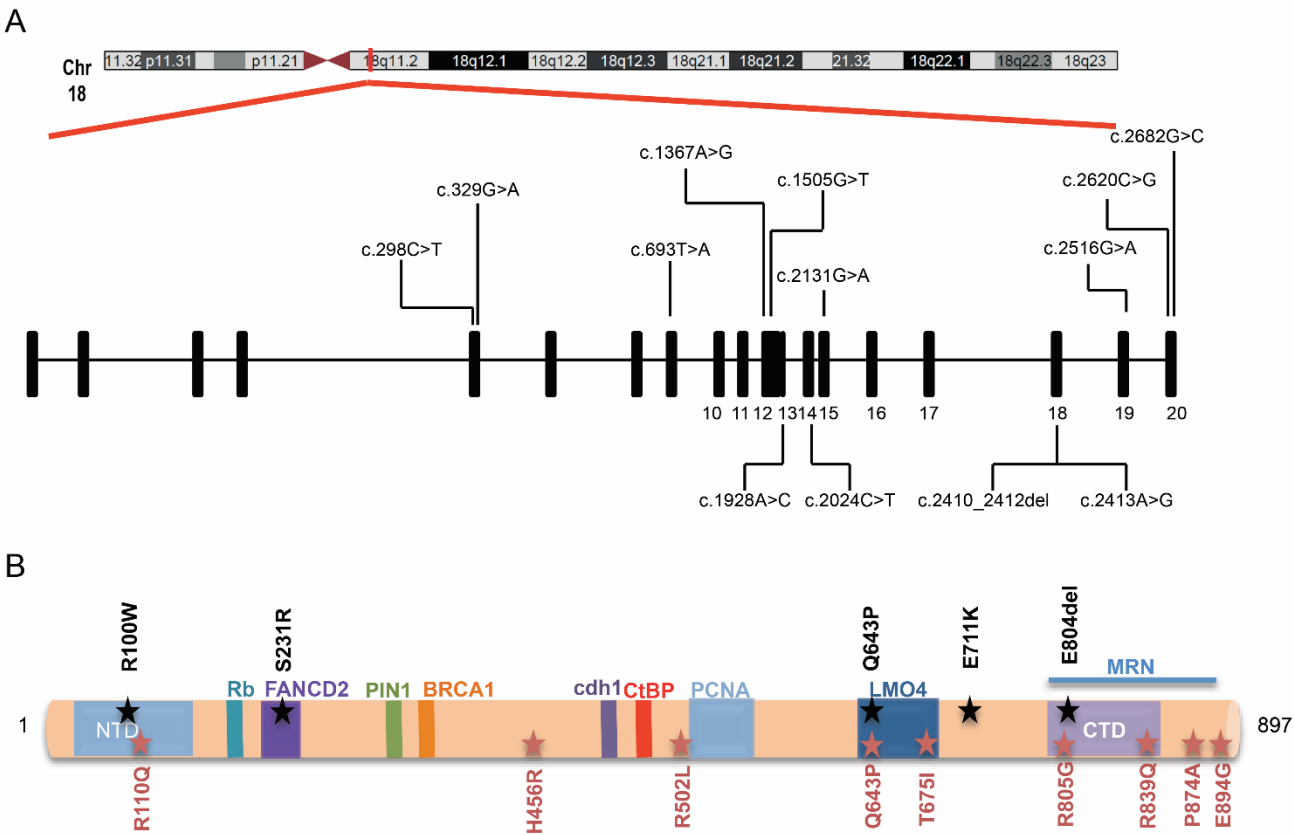


Figure 1. Identification of *RBBP8* germline variants. (A) Schematic representation of the identified variants at gene level indicated according to exon location. (B) Schematic representation of the identified variants at protein level indicated according to known functional domains. The multimerization domain (aa 45-165), the Sae2-like domain (aa 790-897) and the BRCA1 binding site are indicated. All variants further investigated in the functional studies are indicated in bold.

Figure 2. Subset of *RBBP8*/CtIP variants display a genome maintenance defect

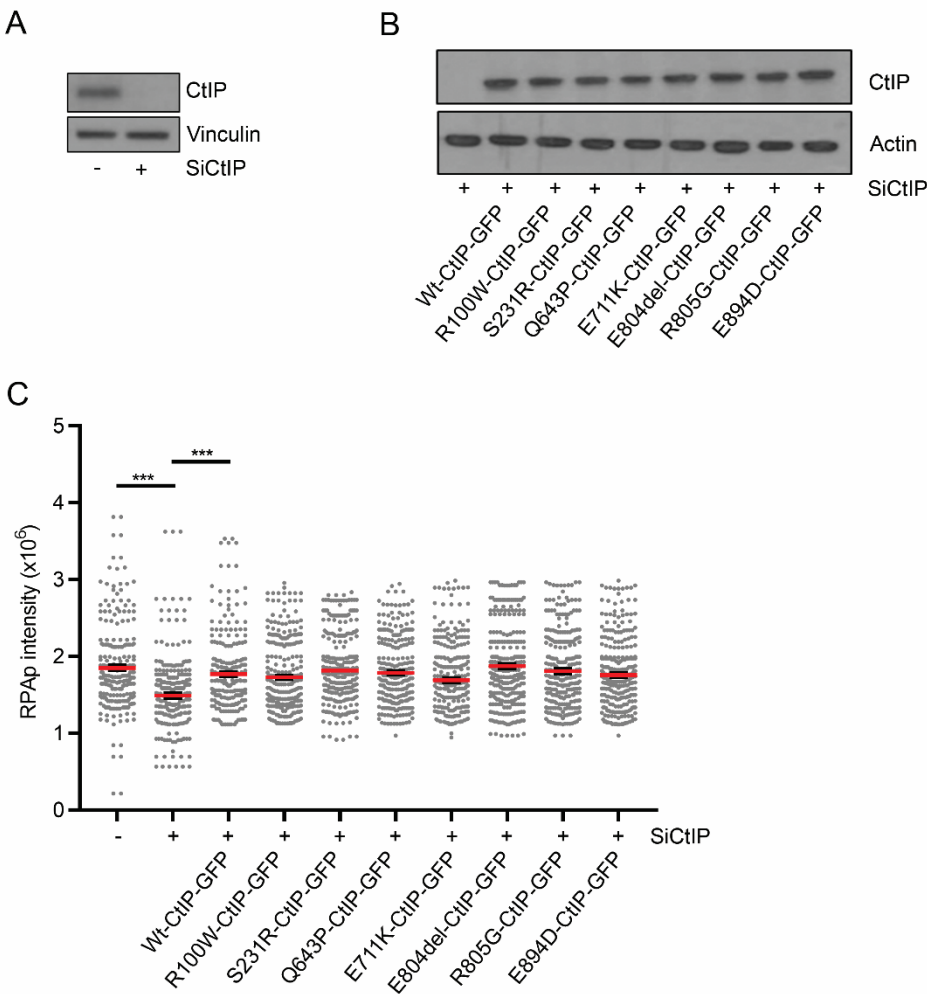


Figure 2. Subset of *RBBP8*/CtIP variants display a genome maintenance defect. (A-B) Western blot analysis of CtIP siRNA, GFP CtIP variants, Actin and Vinculin expression in MCF7 cells. Actin and Vinculin were used as loading controls. (C) The relative intensity of phosphorylated RPA (S4/8) was examined in the total population of Wt or its mutated CtIP variants 3 h post exposure to IR (15 Gy). Cells were fixed and stained for pRPA (S4/8). Each of the variants was compared to Wt-CtIP-GFP, but no significant changes were observed. The displayed data represents three independent biological replicates and per sample $n \geq 280$ nuclei were analyzed. Holm-corrected multiple testing was performed of ranked data fitted by a linear mixed model, comparing all CtIP variants to Wt-CtIP-GFP.

Figure 3. CtIP prevents ssDNA accumulation after replication stress.

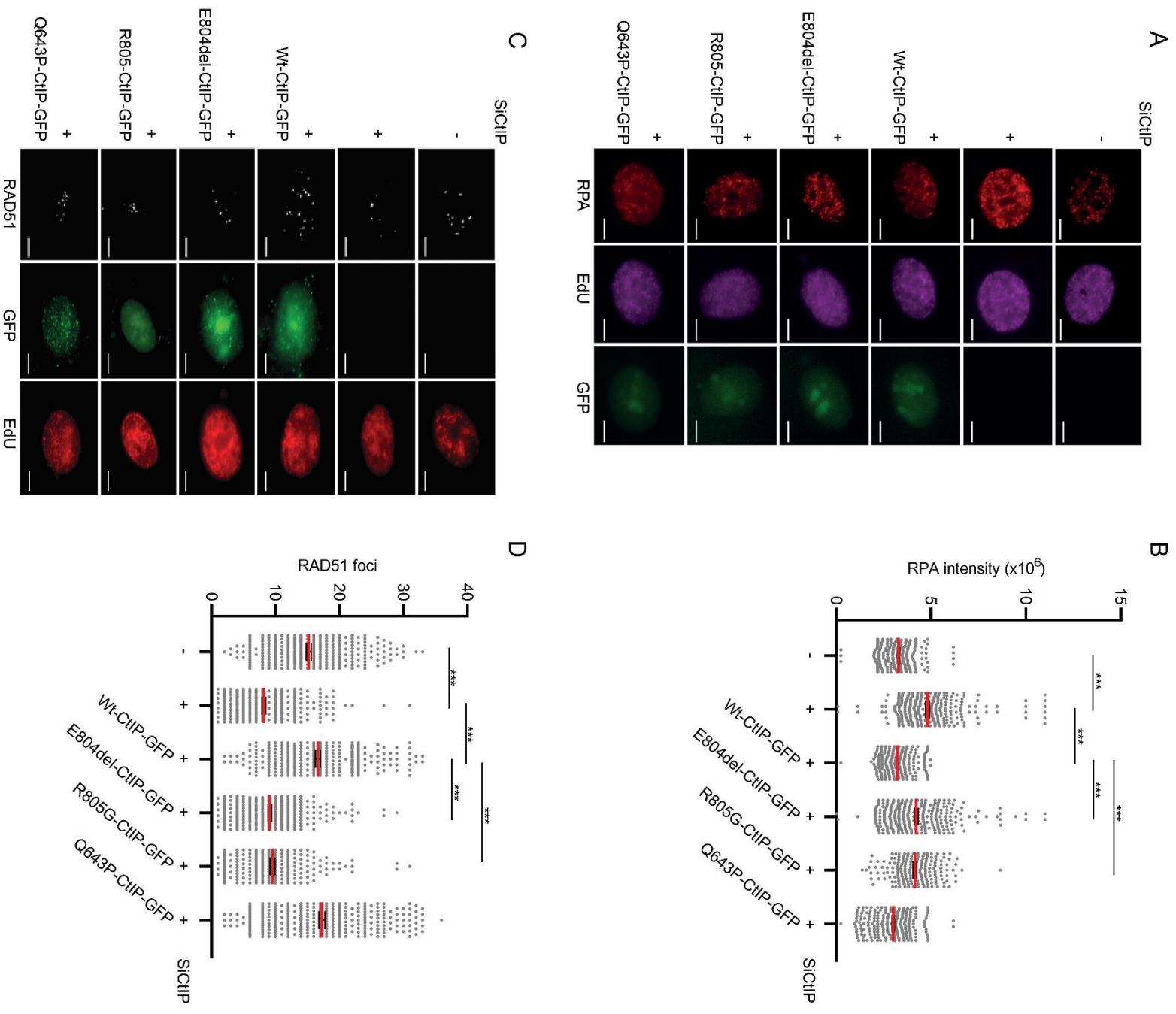


Figure 3: CtIP prevents ssDNA accumulation after replication stress. (A) Representative images displaying RPA in HU-treated EdU-positive cells. Scale bar= 20 μ m. (B) MCF7 cells were transfected with the indicated siRNA and 24 h later, cells were transfected with Wt or its mutated CtIP variants. Afterwards cells were pulsed with 10 μ M EdU for 20 min prior to addition of 4 mM HU. Cells in S phase (EdU+) at the time of HU treatment were Click-IT labeled with an Alexa Fluor 594 azide and RPA intensity in EdU-positive cells were enumerated using Image J/Fiji. The displayed data represents three independent biological replicates and per sample $n \geq 174$ nuclei were analyzed. Holm-corrected multiple testing was performed of ranked data fitted by a linear mixed model, comparing all CtIP variants to Wt-CtIP-GFP. (C) Representative images displaying RAD51 in HU-treated EdU-positive cells. Scale bar= 20 μ m. (D) MCF7 cells were transfected with the indicated siRNA and 24 h later, cells were transfected with Wt or mutated CtIP variants. Afterwards cells were pulsed with 10 μ M EdU for 20 min prior to addition of 4 mM HU. Cells in S phase (EdU+) at the time of HU treatment were Click-IT labeled with an Alexa Fluor 594 azide and RAD51 foci in EdU-positive cells were enumerated using Image J/Fiji. The displayed data represent three independent biological replicates and per sample $n \geq 207$ nuclei were analyzed. Holm-corrected multiple testing was performed of ranked data fitted by a linear mixed model, comparing all CtIP variants to Wt-CtIP-GFP.

Figure 4. CtIP promotes fork protection through FBH1.

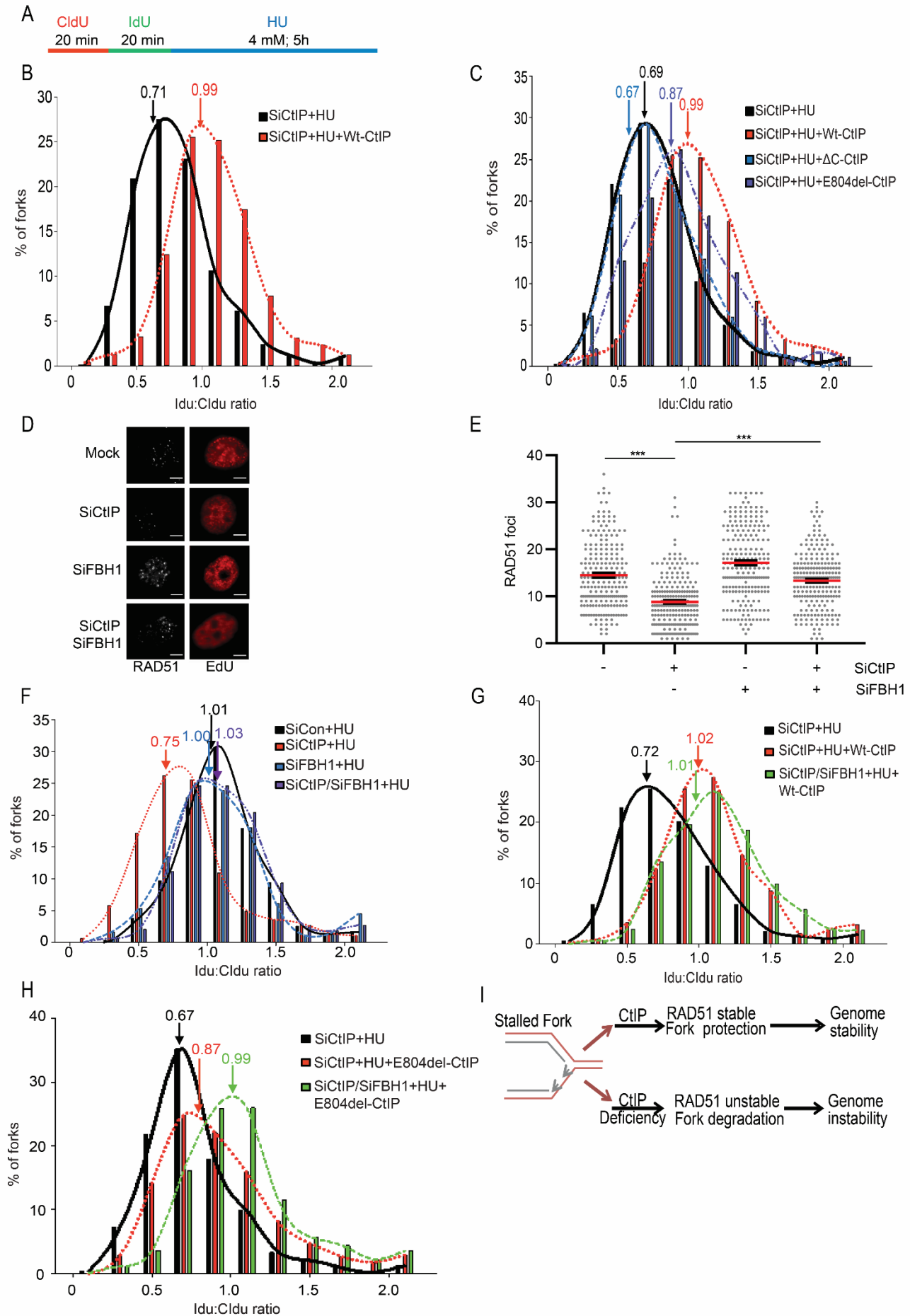


Figure 4: CtIP promotes replication fork protection through FBH1. (A) Experimental scheme of dual labeling of DNA fibres in DOX inducible U-2-OS cells stably expressing the siRNA resistant full-length Wt, E804del or Δ C CtIP. Cells were sequentially pulse-labeled with CldU and IdU, then treated with 4 mM HU for 5 h. (B-C) Loss of CtIP results in replication fork instability in response to replication stress. DOX-inducible U-2-OS cells were transfected with either UNC (negative control) or CtIP siRNA and 24 h later, cells were induced with DOX for 24 h. IdU:CldU ratios are given. (D-E) Representative images displaying RAD51 in HU-treated EdU-positive cells, scale bar= 20 μ m. MCF7 cells were transfected with the indicated siRNAs. Cells were pulsed with 10 μ M EdU for 20 min prior to addition of 4 mM HU. Cells in S phase (EdU+) at the time of HU treatment were Click-IT labeled with an Alexa Fluor 594 azide and RAD51 foci in EdU-positive cells were enumerated using Image J/Fiji. The displayed data represents three independent biological replicates and per sample n=224 nuclei were analyzed. Holm-corrected multiple testing was performed of ranked data fitted by a linear mixed model. (F) U-2-OS cells were transfected with the indicated siRNAs and exposed to 4 mM HU for 5 h. IdU:CldU ratios are given. (G) U-2-OS cells were transfected with the indicated siRNAs and exposed to 4 mM HU for 5 h. IdU:CldU ratios are given. (H) U-2-OS cells were transfected with the indicated siRNAs and exposed to 4 mM HU for 5 h. IdU:CldU ratios are given. (I) Schematic model for the role of CtIP at stalled forks. CtIP regulates RAD51 stability at stalled forks, counteracting the dissolution of the RAD51 filament by FBH1. Loss of CtIP leads to DNA damage accumulation and enhanced chromosomal instability.